Available online at www.sciencedirect.com
ScienceDirect
Journal of Nutritional Biochemistry 21 (2010) 214–226
Journal of Nutritional Biochemistry

Developmental changes in glycolipids and synchronized expression of nutrient transporters in the mouse small intestine

Azusa Yoneshige, Ayano Sasaki, Masao Miyazaki, Naoya Kojima, Akemi Suzuki, Junko Matsuda*

Institute of Glycoscience, Tokai University, Kanagawa 259-1292, Japan.

Received 4 September 2008; received in revised form 1 December 2008; accepted 10 December 2008

Abstract

Small intestinal epithelial cells are rich in characteristic glycosphingolipids (GSLs) that are composed of phytosphingosine and α-hydroxy fatty acid, but the physiological roles of GSLs in the small intestine remain unclear. Here, we report the developmental changes in GSL composition in the mouse small intestine (duodenum through ileum) and their relationship with the temporal mRNA expression of nutrient transporters. Up to 2 weeks after birth, the major GSLs were hexosylceramide (HexCer), GM3, GM1 and GD1a. After 2 weeks of age, HexCer and asialo GM1 became the major GSLs. The ceramide moiety of both HexCer and asialo GM1 was composed mainly of phytosphingosine and α-hydroxy fatty acid, from birth through adulthood. Immunohistochemically, GM1 localized in the cytoplasm, and asialo GM1 localized exclusively in the apical microvillous membrane of small intestinal epithelial cells. The shift from sialylated GSLs to asialo GM1 was achieved by the combinational and tissue-specific transcriptional down-regulation of GM3 synthase and GM1-β-galactosidase at around 2 weeks of age. The temporal mRNA expression of various nutrient transporters also showed significant changes at around 2 weeks of age, including the up-regulation of the sodium/glucose cotransporter and the oligopeptide transporter, as well as the down-regulation of amino acid transporters. These synchronized changes in the mRNA expression of nutrient transporters with GSL composition during suckling-to-weanling transition suggest the contributions of GSLs to morphologic and functional development in the membrane of mouse small intestinal epithelial cells.

Keywords: Glycosphingolipid; Ganglioside; Asialo GM1; Epithelial cell; Microvillous membrane; Microdomain

1. Introduction

The small intestine is a highly developed organ for nutrient digestion and absorption, consisting of villi lined by a single layer of epithelial cells [1,2]. Small intestinal epithelial cells are polarized cells that have the apical microvillous brush border membrane, where many transporter proteins are expressed and active material transport takes place. They are also rich in glycosphingolipids (GSLs), which are amphipathic molecules consisting of a hydrophilic sugar chain and a hydrophobic ceramide moiety, and are components of eukaryotic cell membranes [3,4]. GSLs are segregated into membrane microdomains (rafts) and contribute to membrane protein functions and signal transduction [5,6]. The functions of various transporter proteins on the microvillous membrane are suggested to be supported by microvillous membrane-specific lipid components [5,6].

Thousands of different GSLs have been reported due to the diversity of their headgroup sugar chain, backbone sphingoid base and fatty acid structures. The different carbohydrate headgroups are formed by stepwise reactions of glycosyltransferases [4]. Their expressions are not only cell-specific or tissue-specific, but also regulated during development and differentiation. They are thought to play a role in cellular interactions [7]. Variations within the ceramide moiety are due to different alkyl chain lengths and degrees of hydroxylation and desaturation. Dihydroceramide desaturase (DES1) introduces the *trans*-double bond at C-4 of sphinganine to produce ceramide. Dihydroceramide C-4 hydroxylase (DES2) introduces the hydroxyl group at C-4 of sphinganine to produce phytoceramide [8–12]. α-Hydroxylase introduces the hydroxyl group at the α carbon of fatty acids [13,14]. The distribution of each GSL is unique, depending on tissues, cells and developmental stages [15,16]. In particular, small intestinal epithelial cells have a characteristic hydrophilic ceramide moiety that is composed of phytosphingosine (which carries an additional hydroxyl group at the C-4 position of the sphingoid base) and α-hydroxy fatty acid [17–26]. Phytoceramide production is catalyzed by DES2, which is expressed most abundantly in small intestinal epithelial cells [8–12]. However, the molecular mechanisms of how these characteristic GSLs support the membrane functions of small intestinal epithelial cells remain unclear.

In the present study, to increase our understanding of the biological functions of GSLs in the membrane of small intestinal epithelial cells, we analyzed developmental changes in GSL composition in the postnatal mouse small intestine and their transcriptional regulation by GSL metabolic enzymes. The techniques used include thin-layer chromatography (TLC), both alone and in combination with matrix-assisted laser desorption/ionization quadrupole ion trap time-

* Corresponding author. Tel.: +81 463 58 1211x4644; fax: +81 463 50 2432.
E-mail address: matsujun@keyaki.cc.u-tokai.ac.jp (J. Matsuda).

0955-2863/$ – see front matter © 2010 Elsevier Inc. All rights reserved.
doi:10.1016/j.jnutbio.2008.12.009

of-flight mass spectrometry (TLC-MALDI-QIT-TOF MS). In addition, since the mouse small intestine undergoes an important transformation in nutrient absorption during postnatal development [27], we analyzed the temporal mRNA expression of various nutrient transporters during the suckling, weanling and adult stages, as well as their relationship with the developmental changes in GSL composition.

2. Materials and methods

2.1. Lipid standards

A standard mixture of neutral glycolipids for TLC [GalCer, LacCer, trihexosylceramide (CTH) and globoside] and a crude ganglioside mixture prepared from bovine brain (GM1, GM2, GM3, GD1a, GD1b and GT1) were purchased from IsoSep AB (Tullinge, Sweden). Asialo GM1, prepared from bovine brain GM1, was obtained from Wako Pure Chemical Industries Ltd. (Tokyo, Japan). Asialo GM1 containing phytosphingosine and α-hydroxy fatty acid was purified from mouse small intestine, as described previously [18]. The purified gangliosides GM2 and GM3 were purchased from Matreya LLC (Pleasant Gap, PA, USA).

2.2. Tissues

Mice of C57BL/6J and 129SvEv mixed background were killed, and segments of the gastrointestinal tract, including the stomach, duodenum, jejunum/ileum, appendix and large intestine, along with the whole brain tissue, were collected at 3, 12, 16, 19, 24, 31 and 44 days of age during the suckling, weanling and adult stages. The tissue from the duodenum through the ileum was used as the small intestine. Food debris in the gastrointestinal tissue was washed out by saline for lipid analyses. Tissues derived from more than four mice were collected at each time point, frozen immediately in liquid nitrogen and then stored at −80°C until use for either lipid or RNA extraction. All animals were kept under a conventional environment and maintained under a 12-h light/dark cycle at ambient temperature (23±3°C) with a solid diet (MF from Oriental Yeast Co., Ltd., Tokyo, Japan) and water available ad libitum. Offspring were weaned from their mothers at 21 days of age. This study was carried out in accordance with the Guidelines for the Care and Use of Laboratory Animals adopted by the Committee on Animal Research at Tokai University.

2.3. Lipid analyses

2.3.1. Lipid extraction from tissues

Whole tissues were homogenized with 4 vol of water (wt/vol tissues) by weight in a glass Potter–Elvehjem homogenizer. Lipid extraction with chloroform/methanol (1:2, vol/vol) was performed as described previously [28]. Lipids were fractionated to neutral and acidic fractions using a reverse-phase column (Bond Elut C-18; 3 ml/ 500 mg; Varian, Inc., Palo Alto, CA, USA) in accordance with Kyrklund's method [29], with modifications described previously [30]. Aliquots of the neutral lipid fractions were subjected to a mercuric chloride saponification procedure to remove essentially all of the glycerophospholipids [31].

2.3.2. TLC

Each of the neutral and acidic lipid fractions was dissolved in chloroform/methanol (2:1, vol/vol), and the fractions equivalent to 20 mg of wet tissue weight were applied as 3- to 10-mm spots to silica-gel-coated plates with aluminum backing (Merck, Darmstadt, Germany). Plates were developed with a solvent system of chloroform/methanol/water (65:25:4, vol/vol/vol) for neutral lipids and with a solvent system of chloroform/methanol/0.2% $CaCl_2$ (55:45:10, vol/vol/vol) for acidic lipids. The neutral GSLs or gangliosides were detected by spraying with orcinol or resorcinol reagent and by heating the plates at 120°C or 98°C, respectively. The orcinol-stained spots were scanned using a Fujifilm LAS-3000 imaging system (Fujifilm, Tokyo, Japan) and quantified using Multi Gauge Ver3.0 software (Fujifilm). The protein level of 20 mg of the wet tissue weight of each tissue homogenate was almost identical to that of 10.90 ±0.35 mg of protein (n=7).

2.3.3. TLC immunostaining

TLC immunostaining was performed as described previously [32], with minor modifications. In brief, neutral or acidic GSLs were separated on a TLC plate with aluminum backing on the solvent systems described above. The plate was cut into two pieces, one of which was sprayed with orcinol reagent to determine the positions of the GSLs. The other piece for immunostaining was soaked in 0.1% polyisobutylmethacrylate in cyclohexane for 1 min, dried and preincubated with 1% bovine serum albumin (BSA)–phosphate-buffered saline (PBS) for 30 min. The plate was then incubated with primary antibodies in 1% BSA–PBS: either affinity-column-purified rabbit polyclonal anti-asialo GM1 antibody (prepared from brain GM1; 100 μg/ml immunoglobulin) [18] or mouse monoclonal anti-GM3 antibody (1 μg/ml; Seikagaku Corp., Tokyo, Japan) for 1.5 h at room temperature. The plate was washed with PBS and then incubated with secondary antibody diluted 1:5000 with 1% BSA–PBS: either peroxidase-conjugated anti-rabbit IgG antibody (Roche, Penzberg, Germany) or horseradish-peroxidase-conjugated anti-mouse IgM (Jackson ImmunoResearch Laboratories, Inc., West Grove, PA, USA) for 1 h at room temperature. The plate was washed again with PBS, and the GSL bands were visualized by enhanced chemiluminescence with Super Signal (Pierce, Rockford, IL, USA) using a Fujifilm LAS-3000 imaging system and quantified using Multi Gauge Ver3.0 software. For detection of GM1, peroxidase-conjugated cholera toxin B subunit (CTxB; 100 ng/ml; Calbiochem, Darmstadt, Germany) was used.

2.3.4. TLC mass spectrometry

When samples on a TLC plate were directly analyzed by TLC-MALDI-QIT-TOF MS without staining, duplicate and side-by-side spots were made for each sample, and the plate was cut into two pieces after development. One piece was used as reference for the positioning of GSLs that were detected with orcinol reagent. The other piece was used for TLC-MALDI-QIT-TOF MS as described previously, with some modifications [32,33].

An Axima-QIT mass spectrometer equipped with a nitrogen laser (337 nm, 3 ns pulse width; Shimadzu Corp., Kyoto, Japan) was used as described previously [32]. Mass spectra were assembled from 200 to 1000 accumulations of the profile obtained by two laser shots using a laser power of 30–60 arbitrary units in positive ion mode. Stronger laser power increased the sensitivity of MS and provided fragment ions used as precursor ions for sequential MS/MS analysis. External calibration of the MS spectra was performed using angiotensin II ($[M+H]^+$; m/z=1046.5) and adrenocorticotropic hormone ($[M+H]^+$; m/z=2465.2) (Sigma, St. Louis, MO, USA) on a MALDI sample plate, rather than on a TLC plate. TLC plates for MS analysis were cut into small pieces containing GSLs, and the pieces were attached to a MALDI sample plate with two-sided tape. Several small droplets of freshly prepared matrix solution [0.1 mg/μl 2,5-dihydroxybenzoic acid in acetonitrile/water (1:1, vol/vol)] were then deposited on the spot area using a microsyringe (Hamilton, Reno, NV, USA) with immediate drying using a cold air stream after each droplet.

2.4. Immunohistochemistry

Mice ages 13 and 44 days were anesthetized with ether and perfused through the left cardiac ventricle with physiological saline (0.9% NaCl), followed by 4% paraformaldehyde in 0.1 M sodium phosphate buffer (pH 7.4). Then the small intestine (duodenum through ileum) was dissected, and food debris was washed out with physiological saline. The sample was then embedded into OCT compound (Sakura Finetek USA, Inc., Torrance, CA, USA) after immersion in phosphate buffer containing 30% sucrose until it had settled at the bottom of the container at 4°C and frozen on dry ice. For sectioning, the samples were cut into 6-μm thick slices with a cryostat microtome (Leica, Wetzlar, Germany) and thaw-mounted on glass slides coated with Matsunami adhesive silane (Matsunami, Osaka, Japan).

Frozen sections were rinsed with PBS and then incubated with 1% BSA for 1 h at room temperature, followed by incubation with the primary antibodies: anti-asialo GM1 antibody, anti-sodium/glucose cotransporter (SGLT1) antibody, anti-low-density lipoprotein receptor (LDL-R) antibody and anti-oligopeptide transporter (PEPT1) antibody (Santa Cruz Biotechnology, Inc., Santa Cruz, CA, USA), overnight at 20°C, then finally incubated with the secondary antibodies: fluorescein-isothiocyanate-conjugated donkey anti-rabbit IgG and Cy3-conjugated donkey anti-goat IgG (Jackson ImmunoResearch Laboratories, Inc.) for 2 h at room temperature, followed by DNA staining with Hoechst 33342 as previously described [34]. After the immunostained sections had been rinsed in PBS, they were mounted in Vectashield (Vector Laboratory, Peterborough, UK) and examined by fluorescence microscopy (Keyence, Osaka, Japan) or with a confocal laser scanning microscope (LSM510; Zeiss, Oberkochen, Germany). For detection of GM1, the peroxidase-conjugated CTxB described above was used at a concentration of 20 ng/ml and visualized with diaminobenzidintetrahydroxy chloride.

To confirm the lipid nature of positive staining with anti-asialo GM1 antibody or CTxB, air-dried sections were treated with methanol for 10 min, followed by chloroform/methanol (1:1, vol/vol) for another 10 min, then stained using the same procedure as described above. As negative control for nonspecific staining, additional sections were subjected to the immunostaining procedure without primary antibodies. The experiments were repeated three times using three different sections from different mice.

2.5. Relative quantification of the mRNA expression levels of GSL metabolic enzymes and nutrient transporters by real-time RT-PCR

Total RNA was extracted from mouse small intestine (duodenum through ileum) and whole brain tissue (n=4) at each time point (3, 12, 16, 19, 24 31 and 60 days of age) with TRIzol reagent (Invitrogen, Carlsbad, CA, USA) in accordance with the manufacturer's protocol. Total RNA was treated with DNase (Promega, Madison, WI, USA) then quantified by UV spectrophotometry. The following analysis was performed using 10 μg of RNA: TaqMan reverse transcription reagent and TaqMan universal PCR master mix (Applied Biosystems, Foster City, CA, USA) were used for RT-PCR. The RNA expression of several GSL metabolic enzymes and nutrient transporters that are expressed in the small intestine was quantified using the AB 7500 real-time PCR system (Applied Biosystems). The oligonucleotide primers and FAM-labeled TaqMan universal probes were purchased from Roche. The sequences of the primers and the number of universal probes for each gene are listed in Table 1. The mouse glyceraldehyde-3-

phosphate dehydrogenase (*GAPDH*) gene was used as endogenous control to normalize the amount of total RNA in each sample. The oligonucleotide primers and VIC-labeled TaqMan probe for GAPDH were purchased from Applied Biosystems (TaqMan rodent GAPDH control reagent VIC probe). Relative expression levels were evaluated by relative quantification using SDS v1.3 software (Applied Biosystems). The expression ratio of each gene relative to GAPDH was calculated by $2^{-\Delta\Delta C_t}$ (C_t, threshold cycle). For all primer sets, the kinetics of the PCR was confirmed by serial dilutions of different cDNA preparations. These analyses verified that the efficiencies of amplification were equal for both primer sets, thereby allowing quantification by the comparative C_t method (user bulletin no. 2; Applied Biosystems).

2.6. Statistical analysis

All values are presented as mean±S.E. Statistical analysis was performed using Mann–Whitney *U*-test. Statistical significance was defined as $P<05$.

Table 1
Primers and probes used for real-time RT-PCR

Gene	Primer sequence	Universal probe number	Membrane orientation
(A) Enzymes involved in sphingolipid metabolism			
St3gal5	S: acccagcttgttaataaaagacatc	92	
	A: gcggtgtaattcaaaatgagg		
St3gal2	S: gctctggctatggacaagaag	5	
	A: acagtcggtgcctgattcat		
St8sia1	S: tcgttcaccatcgataattcc	103	
	A: ttcttcaatggcagctgga		
Galnt1	S: acatacgatgctggaatggat	52	
	A: gttcctccacactgccaaat		
Galt4	S: tcagcagcagctggttaaag	10	
	A: tgtgggcacagctgttagag		
Fut2	S: gcggttcgtccattccta	76	
	A: aaaggtacctgggcactcg		
Neu3	S: acgggagagcccagagag	69	
	A: ctgctggaacagggtgct		
Glb1	S: caccttttacgtgggcaac	58	
	A: gccattgatccatacttgacc		
DES1	S: ggctatcataacgagcaccat	60	
	A: cacttgcgatcttcctcacc		
DES2	S: ggttaccacatggaacacca	60	
	A: gcaatcttccgcaccagt		
(B) Nutrient transporters			
Peptide transporter			
PEPT1 (Slc15a1)	S: agctctgatcgcagactcgt	60	Apical
	A: cgtgtagacgatggatagtgaaa		
Amino acid transporter			
EAAT3 (Slc1a1)	S: gctctattaccagaccaactacctg	83	Apical
	A: tgttgaaggggctcagaaac		
NBAT (Slc3a1)	S: ccatgtcaacggtgtaacca	102	Apical
	A: gccagctggagtttccatac		
4F2hc (Slc3a2)	S: caaagtgccaagaaaaagagc	81	Basolateral
	A: ctgagcagggaggaaccac		
y+LAT-1 (Slc7a7)	S: ccagggtcctgtgtttgc	68	Basolateral
	A: atgggggtgtgacttcagc		
LAT2 (Slc7a8)	S: ttactcttatgtgaaggacatcttcg	20	Basolateral
	A: ccagcacagcaatccaca		
ASC-1 (Slc7a10)	S: tggctggaacttcctcaact	17	
	A: gatggcacgaggtaggttct		
Sugar transporter			
SGLT1 (Slc5a1)	S: aagatccggaagaaggcatc	4	Apical
	A: caatcagcacgaggatgaac		
GLUT5 (Slc2a5)	S: gagcaacgatggaggaaaaa	94	Apical
	A: ccagagcaaggaccaatgtc		
GLUT2 (Slc2a2)	S: tgtgatccagtgagtctccaa	75	Basolateral
	A: ggcgcacatctataatgctct		
Fatty acid transporter			
FABP1	S: ccatgactggggaaaaagtc	11	Apical
	A: gcctttgaaagttgtcaccat		
FABP2	S: acggaacggagctcactg	17	Apical
	A: ttaccagaaacctctcggaca		
Others			
mNaDC-1 (Slc13a2)	S: gtcctcttcctgggtgtcaa	60	Apical
	A: gcctgcttccgttcctct		
LDL-R	S: gatggctatacctacccctcaa	64	Basolateral
	A: tgctcatgccacatcgtc		
Na^+/K^+-ATPase (ATP1a1)	S: cttggagaacgtgtgctaggt	10	Basolateral
	A: ttcgggaaactgttcgtca		

St3gal5: GM3 synthase; St8sia1: GD3 synthase; Galnt1: UDP-*N*-acetylgalactosamine:polypeptide *N*-acetylgalactosaminyltransferase 1; Galt4: UDP-Gal:βGalNAc β-1,3-galactosyltransferase 4; Glb1: galactosidase β 1.
PEPT1: solute carrier family 15, member 1; EAAT3: solute carrier family 1 (neuronal/epithelial high-affinity glutamate transporter, system Xag), member 1; NBAT: solute carrier family 3, member 1; 4F2hc: solute carrier family 3 (activators of dibasic and neutral amino acid transport), member 2, CD98 antigen; y+LAT-1: solute carrier family 7 (cationic amino acid transporter, y+ system), member 7; LAT2: solute carrier family 7 (cationic amino acid transporter, y+ system), member 8; ASC-1: solute carrier family 7 (cationic amino acid transporter, y+ system), member 10; SGLT1: solute carrier family 5, member 1; GLUT5: solute carrier family 2 (facilitated glucose transporter), member 5; GLUT2: solute carrier family 2 (facilitated glucose transporter), member 2; FABP1: liver; FABP2: fatty acid binding protein 2, intestinal; mNaDC-1: solute carrier family 13, member 2.

3. Results

3.1. Developmental changes in GSL composition in the mouse small intestine

Each segment of the gastrointestinal tract (stomach, duodenum, jejunum/ileum, appendix and large intestine) in adult mice showed a different GSL composition (Fig. 1). In the small intestine (duodenum, jejunum and ileum), hexosylceramide (HexCer) and asialo GM1 were the major neutral GSLs found. Dihexosylceramide (CDH), globoside and Forssman antigen were also detected at lower levels. Fucosyl asialo GM1 was detected in the jejunum and ileum, but not in the duodenum. These observations were almost identical with a previous report by Umesaki et al. [18,35,36] and Umesaki [37] in the adult mouse of the ICR strain (Fig. 1). The new and interesting finding was that asialo GM1 was characteristic of the small intestine and was barely detectable in other parts of the gastrointestinal tract, including the stomach, appendix and large intestine (Fig. 1). Regarding acidic GSLs, a small amount of GM3 was detected in the adult small intestine (Fig. 1). The band migrating between GM2 and GM3, detected by the orcinol reagent, was not detected by resorcinol reagent, suggesting that this was not a ganglioside, but possibly a sulfated GSL (Fig. 1). In the stomach, HexCer was the major GSL, and globoside and Forssman antigen were also detected to a lesser degree. In the large intestine, HexCer and CTH were the major GSLs, while globoside, Forssman antigen and fucosyl asialo GM1 were also detected.

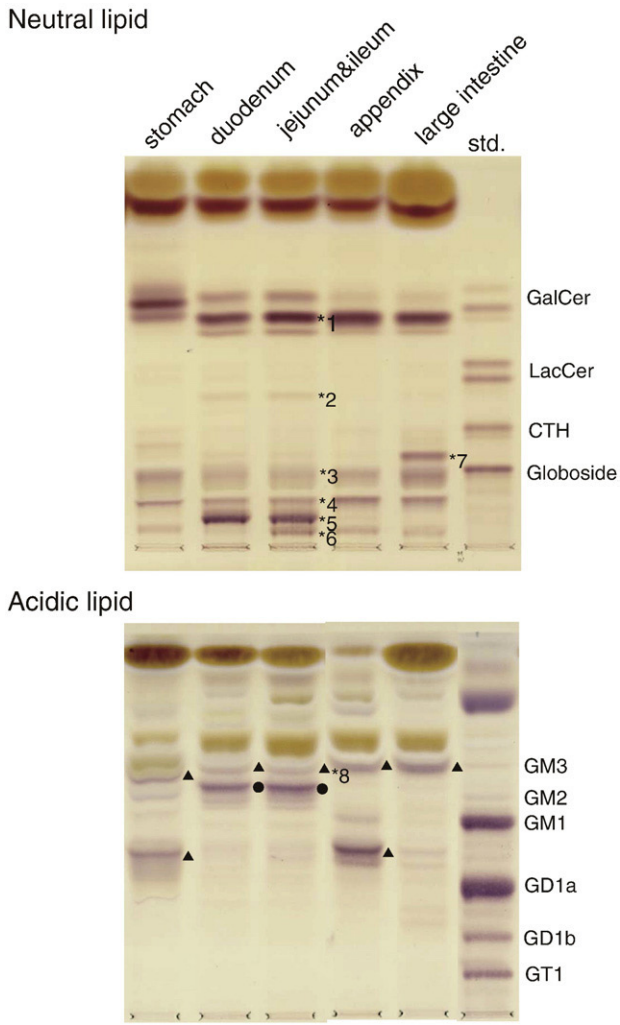

Fig. 1. TLC of neutral and acidic lipids in the gastrointestinal tract of adult mice. Neutral and acidic lipid fractions extracted from the tissues of the gastrointestinal tract, equivalent to 20 mg of wet weight from a 44-day-old mouse, were applied to the plate. The solvent system used was chloroform/methanol/water (65:25:4, vol/vol/vol) for the neutral lipid fraction and chloroform/methanol/0.2% $CaCl_2$ (55:45:10, vol/vol/vol) for the acidic lipid fraction. Detection was achieved using the orcinol reagent. In the neutral lipid fraction, asialo GM1 containing phytosphingosine and α-hydroxy fatty acid (indicated by *5) was characteristically detected in the duodenum through the ileum. In the acidic lipid fraction, a small amount of GM3 was detected in the duodenum through the ileum. In addition to the resorcinol-positive bands (▲) of gangliosides, an undetermined resorcinol-negative but orcinol-positive band (●), which migrated between GM2 and GM3, was detected in the duodenum, jejunum and ileum, suggesting that this was not a ganglioside but possibly a sulfated GSL. Assignments of the detected bands based on our own data by immuno-TLC, TLC-MS and previous reports were as follows: (*1) HexCer; (*2) CDH; (*3) globoside; (*4) Forssman glycolipid; (*5) asialo GM1; (*6) fucosyl asialo GM1; (*7) CTH; (*8) GM3.

The developmental changes in the GSL composition of the small intestine were analyzed from the early neonatal period to adulthood (3–60 days of age). In neonatal mice up to 2 weeks after birth, HexCer was the major neutral GSL. Asialo GM1, which was a major GSL along with HexCer in adult mice, was barely detectable at this age. After 2 weeks of age, asialo GM1 appeared and increased to the level of adult mice at around 3 weeks of age (Fig. 2A). TLC immunostaining results using anti-asialo GM1 antibody revealed that asialo GM1 was not detectable on day 12, but started to appear on day 16 and increased by about 11 fold on day 24 compared to that on day 16 (Fig. 2A). After weaning at around 3 weeks of age, fucosyl asialo GM1 increased and was about fivefold higher on day 24 than on day 12 (Fig. 2A). The amount of HexCer was fairly constant throughout the early neonatal period to adulthood. Throughout this period, both HexCer and asialo GM1 from the small intestine migrated more slowly on a TLC plate than the GalCer and asialo GM1 standards, which were prepared from bovine brain. This has been observed previously in adult mice [17–26], in which the GSLs in the small intestine were composed of phytosphingosine and α-hydroxy fatty acid, a characteristic ceramide moiety with two additional hydroxyl groups from the early neonatal period. Concerning the acidic GSLs, up to 2 weeks after birth, GM1 and GM3 were the major gangliosides, as confirmed by TLC immunostaining (Fig. 2B). After 2 weeks of age, the amounts of GM3 and GM1 decreased markedly and reached the level of adult mice. In contrast, possibly sulfated GSLs became detectable on day 16 and increased markedly on day 19 (Figs. 1 and 2B). After weaning at around 3 weeks of age, the GSL composition was basically fixed through adulthood.

TLC-MS analysis revealed that the ceramide moiety of the neutral GSLs, including HexCer, asialo GM1 and fucosyl asialo GM1 in the small intestine, was composed mainly of phytosphingosine (t18:0) and α-hydroxy fatty acid (hC24:0, hC24:1, hC23:0, hC22:0, hC20:0 and hC16:1) from birth through adulthood (Fig. 3). HexCer, migrating faster in the stomach than in the small intestine, was composed mainly of sphingosine (d18:1) and α-hydroxy fatty acid. In the large intestine, HexCer, CTH and fucosyl asialo GM1 were composed mainly of phytosphingosine (t18:0) and α-hydroxy fatty acid (data not shown).

3.2. Immunohistochemical localization of asialo GM1 in the small intestine

Since asialo GM1 was a characteristic GSL in the small intestine and also appeared at a certain time point during neonatal development, the tissue distribution of GM1 and asialo GM1 in the small intestine (duodenum, jejunum and ileum) was studied by immunohistochemical staining using CTxB and an anti-asialo GM1 antibody. The immunohistochemical localizations of GM1 and asialo GM1 were almost identical through the duodenum to the ileum (data not shown). In the jejunum at 12 days of age, intense staining of GM1 by

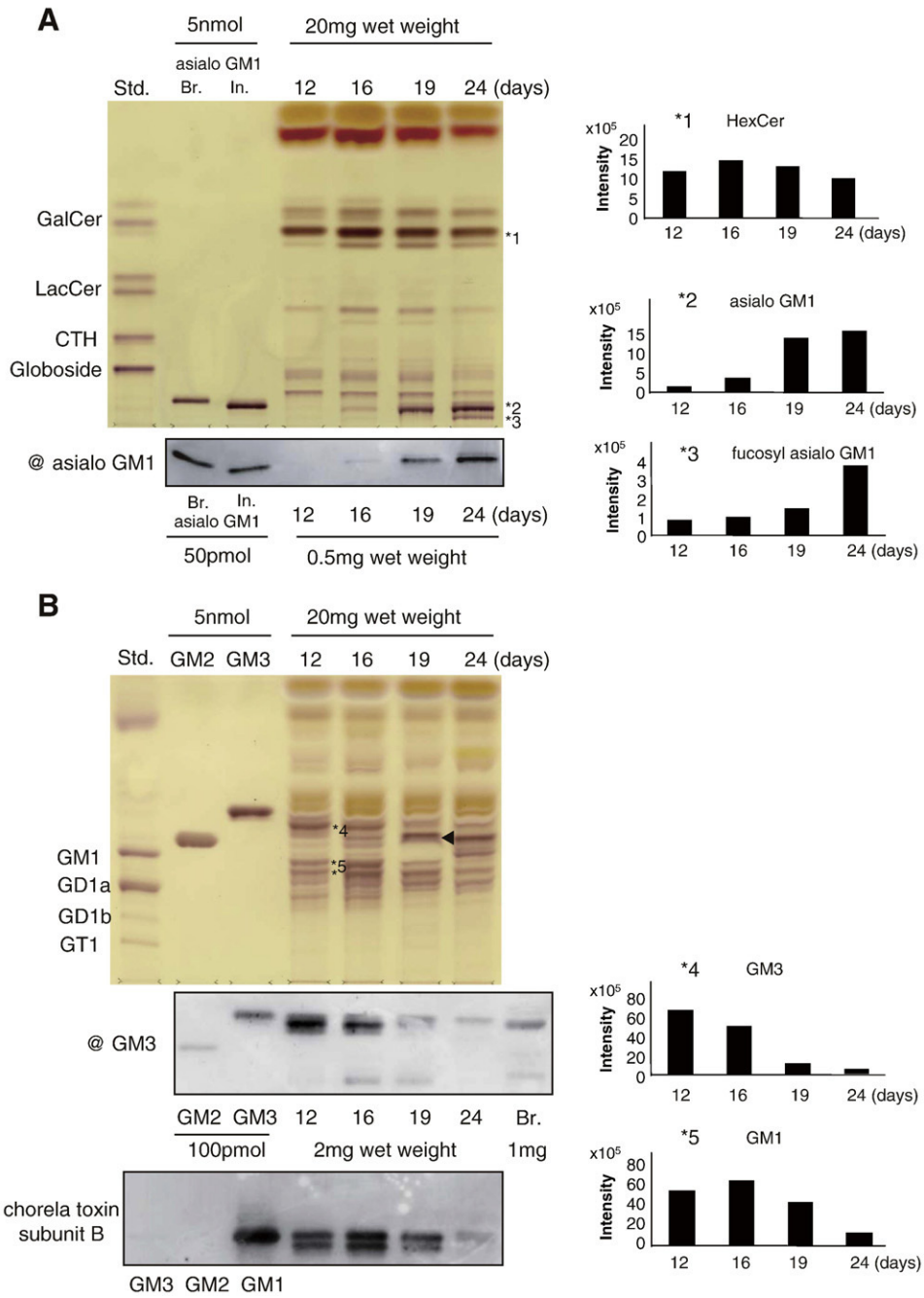

Fig. 2. Developmental changes in the GSL composition of the mouse small intestine. (A) TLC of neutral glycolipids of the small intestine (duodenum through ileum) at different ages. Solvent system, detection reagent and standard glycolipids were the same as in Fig. 1. Asialo GM1 from bovine brain and mouse intestine were also included for reference. The band of *2 was confirmed as asialo GM1 with immune-TLC using an anti-asialo GM1 antibody. The appropriate amount of lipids was applied as described. Before 12 days, HexCer (*1) was the major neutral glycolipid, and asialo GM1 (*2), which was the major and characteristic glycolipid in the adult small intestine, was not detected. Asialo GM1 appeared at around 16 days and increased to the adult level at around 24 days. Fucosyl asialo GM1 (*3) appeared at around the weanling period. The right column presents the quantification of orcinol-detected bands of *1 (HexCer), *2 (asialo GM1) and *3 (fucosyl asialo GM1). The column shows the constant presence of HexCer throughout the neonatal period and a dramatic elevation in asialo GM1 levels after 2 weeks, followed by the induction of fucosyl asialo GM1. (B) TLC of acidic GSLs of the small intestine at different ages. The solvent system used was chloroform/methanol/0.2% $CaCl_2$ (55:45:10, vol/vol/vol). Detection was achieved using the orcinol reagent. The standard gangliosides derived from bovine brain contained GM1, GD1a, GD1b and GT1. Purified GM2 and GM3 were also used for reference. At 12 days, GM3 (*4) and GM1 (*5) were detected as major gangliosides. These gangliosides began to decrease at around 19 days and were almost undetectable at 19 days after weaning. The right column presents the quantification of immune-TLC bands for GM3 and GM1 and shows the decrease in these gangliosides over time. The bands indicated by an arrowhead are possibly sulfated GSLs that were orcinol-positive but resorcinol-negative.

CTxB was detected in the cytoplasm of small intestinal epithelial cells. The staining was more intense in epithelial cells at the villous portion than in crypt cells (Fig. 4B). This gradient distribution of GM1 is consistent with a previous study reporting that GM3 was located in the upper two thirds of the villous and much less in crypt cells in rats [40,41]. The staining by anti-asialo GM1 antibody was barely detectable at this age (Fig. 4C). In the jejunum at 44 days of age, staining by CTxB was barely detected in epithelial cells (Fig. 4E). The anti-asialo GM1 antibody staining of the antigen was clear and intense in the apical brush border membranes of epithelial cells (Fig. 4F and

G). Basolateral membranes of the epithelial cells were also stained, albeit with much less intensity. These tissue distributions of asialo GM1 are in agreement with previous reports on the adult mouse small intestine [19,20]. After the treatment of the sections with organic solvents, almost all these stains were abolished (data not shown). The immunohistochemical results confirm the developmental changes in the GSLs of the neonatal small intestine and indicate that not only the composition but also the localization of GSLs changes at around 2–3 weeks of age in small intestinal epithelial cells.

3.3. Developmental changes in the mRNA expression of enzymes involved in the GSL metabolic pathway

To elucidate the mechanism of these developmental changes in the GSL composition of the small intestine, we compared the temporal expression of GSL metabolic enzymes in the small intestine to that in the brain using real-time RT-PCR techniques (Table 1, Fig. 5). The expression of GM3 synthases ST3 β-galactoside α-2,3-sialyltransferase 5 (St3gal5) and ST3 β-galactoside α-2,3-sialyltransferase 2 (St3gal2) decreased significantly between days 12 and 16. The expression of GD3 synthases ST8 α-*N*-acetylneuraminide α-2,8-sialyltransferase 1 (St8sia1) and GM1-β-galactosidase (Glb1) decreased significantly between days 16 and 19. In addition, DES1 decreased significantly between 16 and 19 days of age, and neuraminidase 3 (Neu3) decreased significantly between 19 and 24 days of age. These findings suggest that the developmental changes in GSL composition were achieved by the combinational down-regulation of GSL metabolic enzymes, including St3gal5, St3gal2, St8sia1 and Glb1, causing the timely conversion from GM3, GM1 and GD1a into asialo GM1, and the induction of asialo GM1 before the weanling period. In particular, since GM3 is the product of St3gal5 catalysis and since asialo GM1 is the substrate of Glb1, the synchronized reduction in the mRNA expressions of St3gal5 and Glb1 at around 12–19 days of age might be the key factor for the induction of asialo GM1 (Fig. 5). In contrast, fucosyltransferase 2 (Fut2) expression tended to increase between 19 and 24 days of age (P=.08), which may cause the induction of fucosyl asialo GM1 after the weanling period [42,43]. In addition, the significant reduction in DES1 compared to DES2 may cause a relative increase in characteristic GSLs with phytosphingosine in small intestinal epithelial cells [11]. In the brain tissues, however, the expression level and the pattern of temporal changes in the GSL metabolic enzymes were different from those observed in the small intestine (data not shown). Although its expression level was relatively low in the brain compared to that in the small intestine, a significant increase in DES2 expression was detected, and further analysis of hydroxylated GSLs in the brain is needed.

3.4. Developmental changes in the mRNA expression of nutrient transporters

As shown by our immunohistochemical data from the small intestine, the microvillous membrane, in which active material transport occurs through various nutrient transporters, is rich in asialo GM1. To clarify the relationship between the developmental changes in GSL composition and the expression of intestinal nutrient transporters, we analyzed the temporal expression of various nutrient transporters (Table 1, Fig. 6). Between 16 and 24 days of age, during which time the developmental changes in GSL composition occur, PEPT1, SGLT1, glucose transporter 5 (GLUT5), sodium-dependent dicarboxylate transporter (NaDC-1) and Na^+/K^+-ATPase α1 subunit (ATP1a1) were up-regulated. In contrast, fatty acid

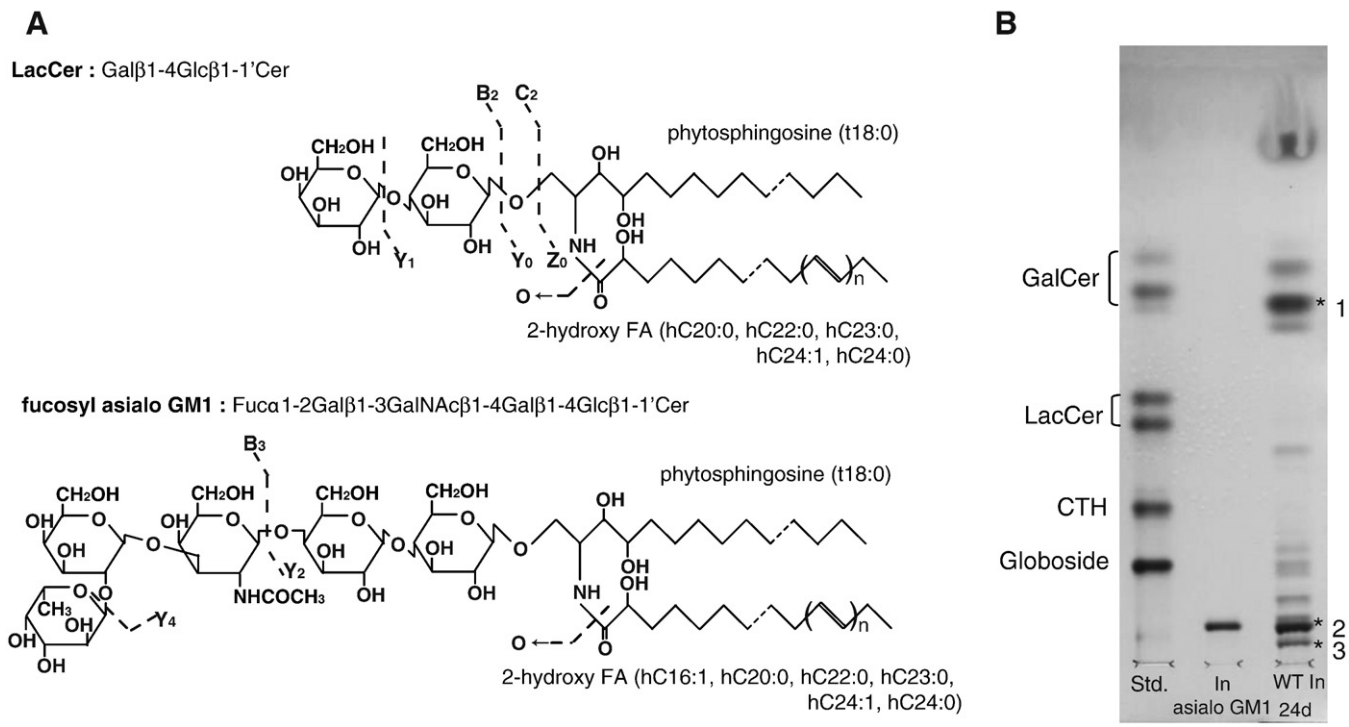

Fig. 3. TLC-MS analysis of neutral GSLs from mouse intestinal tissues. (A) Molecular structure and fragmentation pattern of LacCer and fucosyl asialo GM1. The annotation of fragment ions is in accordance with the nomenclature of Domon and Costello [38], and that of sphingosine is based on the nomenclature of Hsu et al. [39]. (B) Neutral lipid fractions equivalent to 20 mg of wet weight, extracted from the tissues of the small intestine of a 24-day-old mouse, were applied to a plate and then analyzed by MALDI-QIT-TOF MS/MS. MS and MS/MS spectra for (C) HexCer, (D) asialo GM1 and (E) fucosyl asialo GM1. Asterisks indicate the characteristic fragment ions produced by fragmentation of GSLs at the O position, as shown in (A).

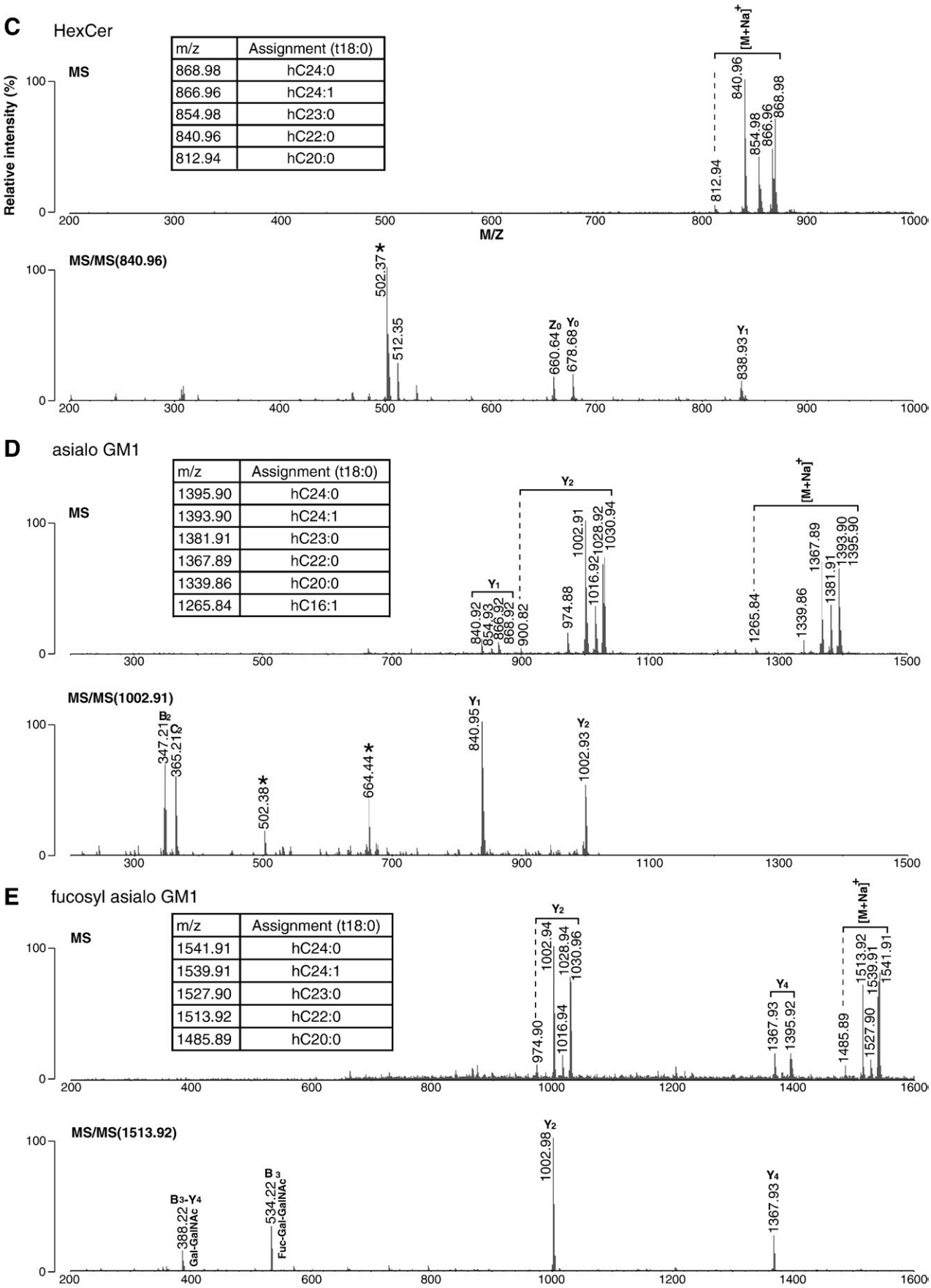

Fig. 3 (*continued*).

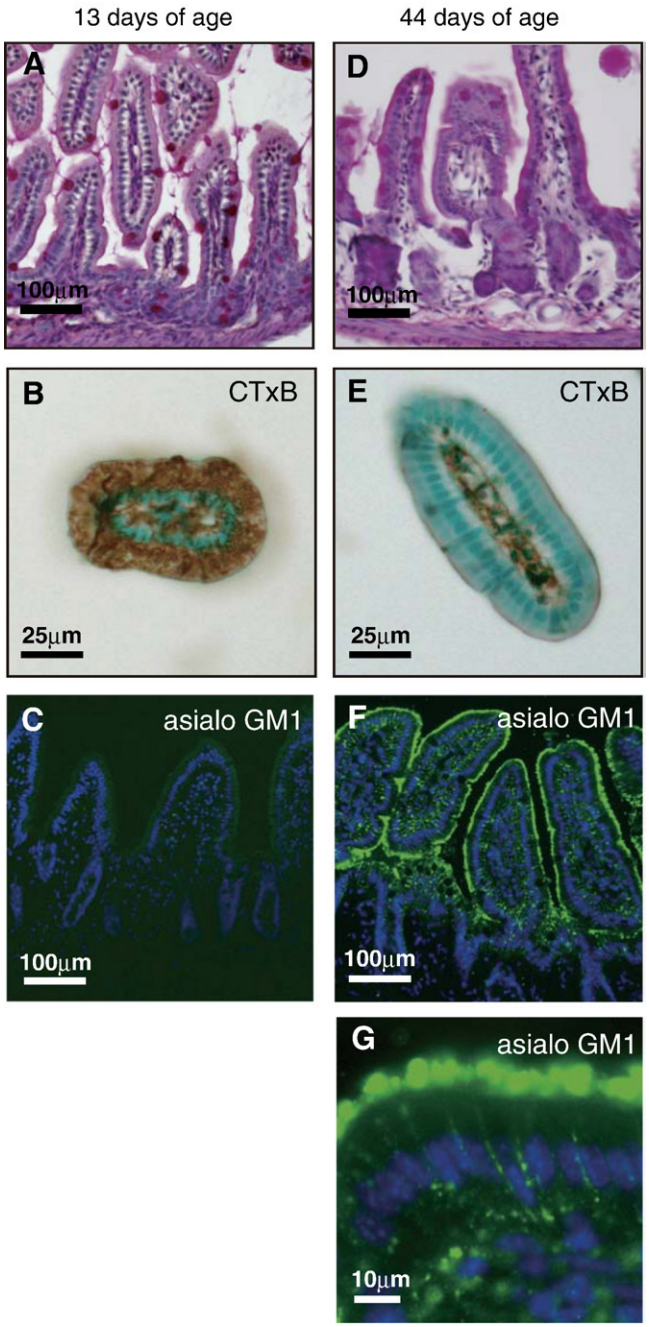

Fig. 4. Immunohistochemical localization of GM1 and asialo GM1 in the neonatal mouse small intestine. In the small intestine (jejunum) at 12 days (A–C), intense CTxB-positive staining (brown) was detected in epithelial cells (B). In contrast, no immunoreactivity of asialo GM1 (green) was observed (C). In the small intestine at 44 days (D–G), weak CTxB-positive staining was detected in mesenchymal cells, but not in epithelial cells (E). In contrast, immunoreactivity of asialo GM1 was observed exclusively in epithelial cells throughout the villi (F). Under higher magnification, it was localized predominantly on the microvillous apical membrane of epithelial cells (G). (A and D) Periodic acid–Shiff and hematoxylin staining. Scale bars represent 100 μm in (A), (C), (D) and (F); 25 μm in (B) and (E); and 10 μm in (G).

binding protein 1 (FABP1), several amino acid transporters (EAAT3, y+LAT-1 and ASC-1), glucose transporter 2 (GLUT2) and LDL-R tended to be down-regulated.

To confirm whether these changes in mRNA expression translate into altered protein expression, we analyzed the expression of SGLT1 and LDL-R by immunohistochemical methods. For SGLT1, at the age of 13 days, the immunoreactivity of SGLT1 was detected mainly in the perinuclear area of epithelial cells (Fig. 7A–C). At the age of 44 days, SGLT1 detection became intense on the microvillous apical membrane of epithelial cells, which was colocalized with the expression of asialo GM1 (Fig. 7D–F). For PEPT1, at the age of 13 days, immunoreactivity of PEPT1 was hardly detected in epithelial cells (Fig. 7G and H). At the age of 44 days, the intense immunoreactivity of PEPT1 was observed on the microvillous apical membrane of epithelial cells (Fig. 7I and J). Since both antibodies to PEPT1 and asialo GM1 were raised by rabbit, we could not perform multiple immunostaining. However, PEPT1 seemed to colocalize with asialo GM1 on the microvillous apical membrane of epithelial cells. For LDL-R, immunoreactivity was more intense at 13 days of age (Fig. 7K–M) than at 44 days (Fig. 7N–P), at which time it was detected on the basolateral membrane of epithelial cells and had not colocalized with the asialo GM1.

4. Discussion

In the present study, we investigated the developmental changes in the GSL composition of the mouse small intestine using TLC and TLC-MS during the suckling, weanling and adult stages. The correlation of these changes with the temporal mRNA expression of GSL metabolic enzymes and intestinal nutrient transporters was examined. We found that the conversion of GSL compositions from HexCer, GM3, GM1 and GD1a into HexCer and asialo GM1 occurs at around 2 weeks of age. The ceramide moiety of HexCer and asialo GM1 was composed mainly of phytosphingosine and α-hydroxy fatty acid from the early neonatal period through adulthood. The immunohistochemical localizations of GM1 and asialo GM1 were different in developing enterocytes. GM1 was localized in the cytoplasm, while asialo GM1 was found exclusively in the apical microvillous membrane. The combinational and abrupt transcriptional down-regulation of GSL metabolic enzymes, including GM3 synthase and Glb1, at around 2 weeks of age is the cause of the timely conversion from GM3, GM1 and GD1a into asialo GM1, and the temporal mRNA expression of various intestinal nutrient transporters changes significantly at around 2 weeks of age.

Based on a study of various adult mammals, the ceramide moiety of GSLs in the mammalian small intestine is commonly composed of a characteristic hydrophilic ceramide species with phytosphingosine and α-hydroxy fatty acid. In contrast, carbohydrate headgroups of GSLs are variable among species. In humans, the small intestine contains sulfatide as a major acidic GSL, with HexCer and CTH as major neutral GSLs [21,25]. In monkeys, GM3, GM2 and GD1a are the principal gangliosides, and CDH is a major neutral GSL [26]. In rats, GM3 is a principal acidic GSL, and HexCer and CTH are major neutral GSLs [22,23]. In mice, Umesaki et al. reported that HexCer and asialo GM1 were the major GSLs in small intestinal epithelial cells. They also demonstrated by subcellular fractionation and immunohistochemical analyses that asialo GM1 is localized mainly in the microvillous membrane of enterocytes [18–20].

Few studies have investigated the developmental changes in GSLs at the early embryonic or neonatal stages of mammals. Developmental changes in rat intestinal GSLs were studied by Bouhours and Bouhours [44,45] and Bouhours et al. [46], in which they found that GM3 was a major ganglioside during the first 2 weeks of life, reaching a maximum concentration at 6 days and decreasing abruptly over following 2 weeks. In contrast, HexCer was a major neutral GSL throughout the perinatal period, and CTH increased after 2 weeks of age. Developmental changes in mouse intestinal GSLs were studied by Sato et al. They found that GM3, GM1 and GD1a were major gangliosides during the suckling period and decreased after the weanling stage, at around 3 weeks of age

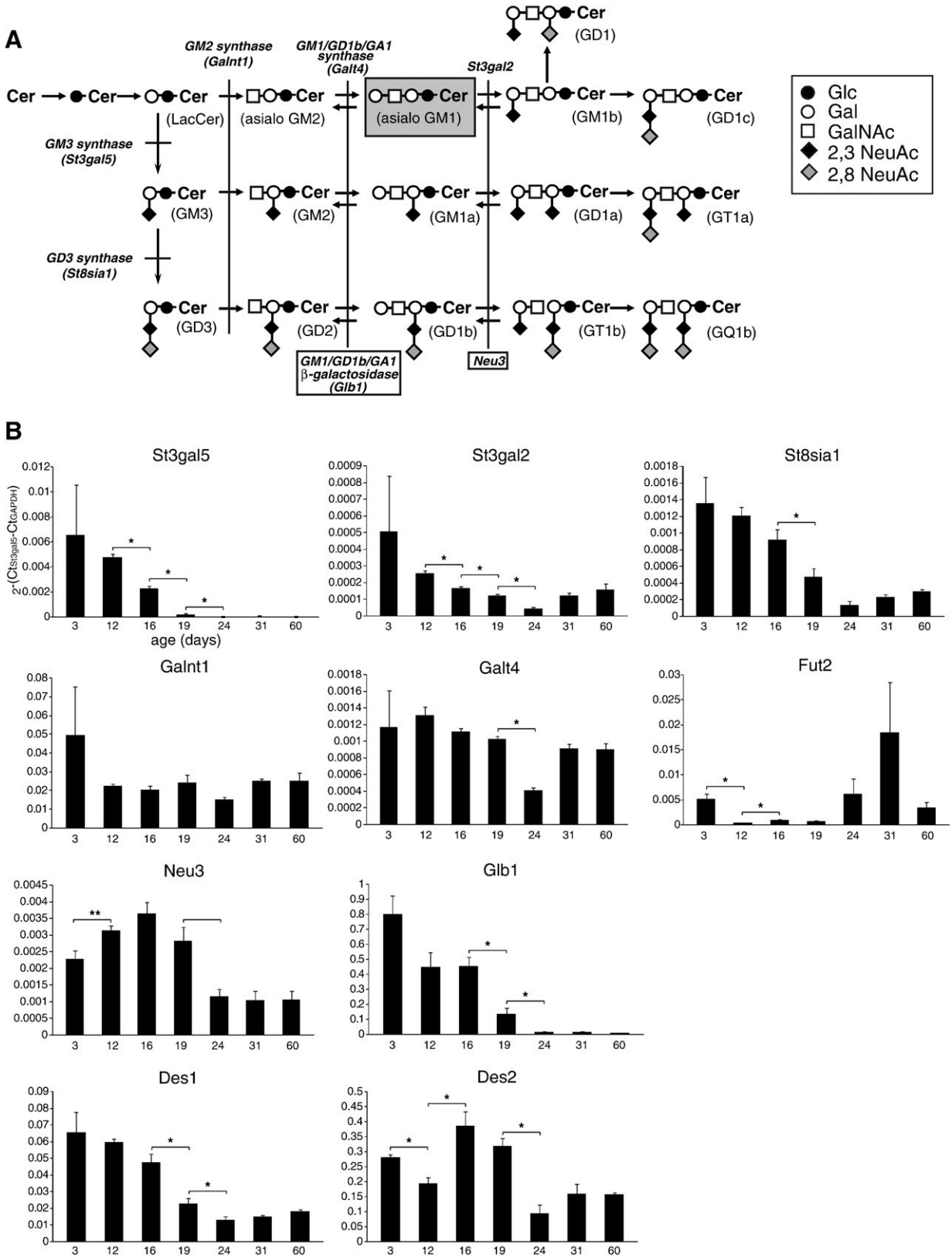

Fig. 5. Temporal changes in the mRNA expression of GSL metabolic enzymes in the small intestine of neonatal mouse. (A) Scheme of the major ganglioside metabolic pathway in mammals. Enzymes in the synthetic pathway are indicated by italics, and enzymes in the degrading pathway are surrounded by an open square. (B) Temporal mRNA expression of GSL metabolic enzymes in the small intestine and brain. The genes examined are listed in Table 1. Expression at each time point (n=4) was calculated by the relative expression ratio of each gene to GAPDH in each sample. Asterisk represents a significant difference between each group (P<.05).

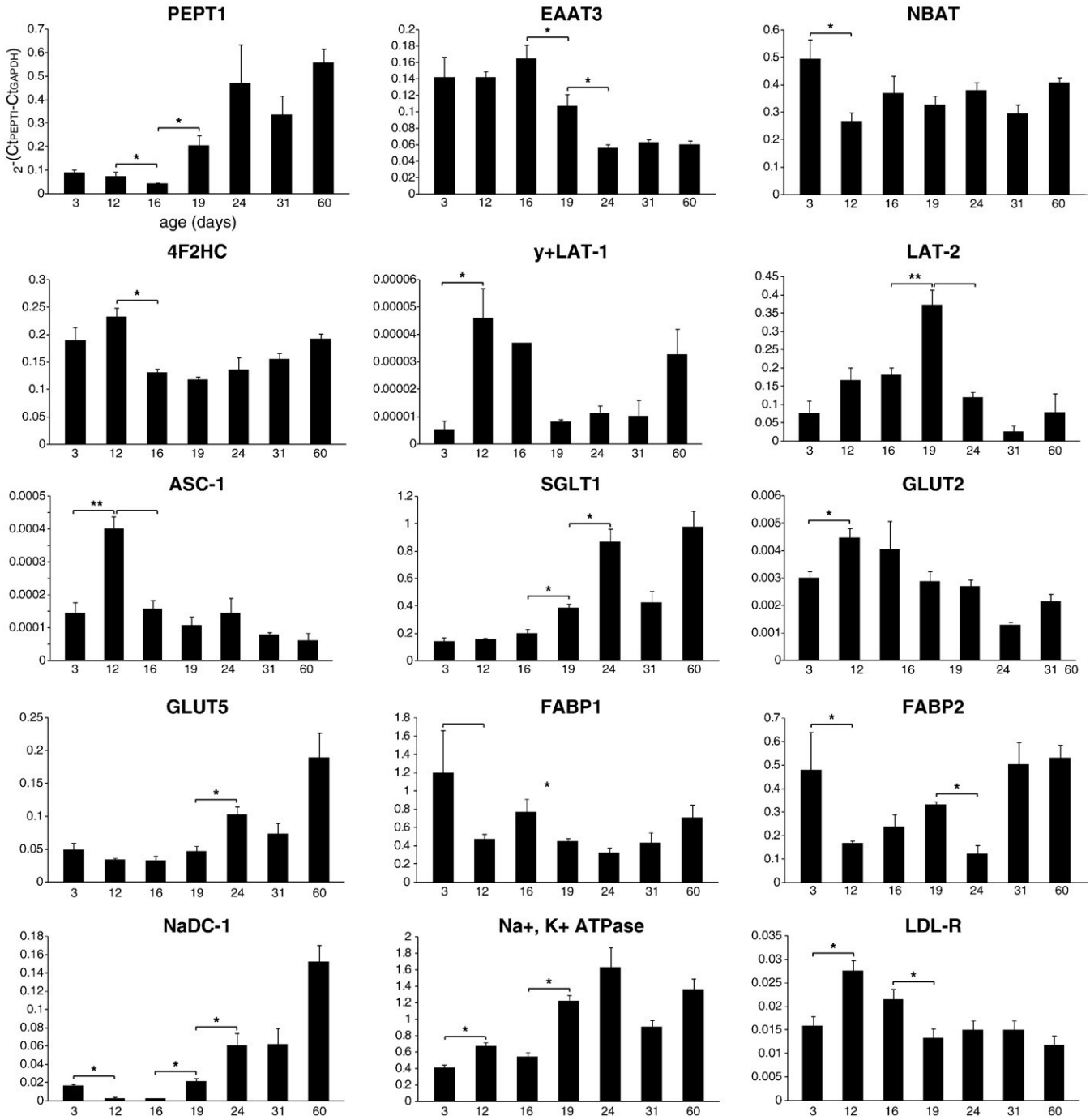

Fig. 6. Temporal changes in the mRNA expression of various nutrient transporters in the small intestine. The genes examined are listed in Table 1. Expression at each time point (n=4) was calculated by the relative expression ratio of each gene to GAPDH. Asterisk indicates a significant difference between groups (P<.05).

[47,48]. Our study showed that the content of gangliosides was high in the early neonatal period and decreased abruptly after 2 weeks. Moreover, this abrupt decrease was synchronized with a marked increase in asialo GM1 after 2 weeks of age. Comparing these developmental changes in mice with those in rats, they could be characterized essentially by a shift from sialylation to asialylation of GSLs at around 2 weeks of age. These developmental changes in GSL glycosylation at the time of sucking-to-weanling transition are similar to developmental changes in glycoprotein glycosylation, which is characterized by a shift from sialylation to fucosylation around the weanling period, also depending on the transcriptional regulation of the corresponding glycosyltransferases [49]. However, a significant increase in possibly sulfated GSL after 2 weeks of age in mice may correspond to the presence of sulfatide in adult humans. The biological function of sulfated GSL in the small intestine might be another point of interest.

How were these developmental changes in GSL composition accomplished in the mouse small intestine? Expression of gangliosides is maintained by stepwise reactions of glycosyltransferases, sialyltransferases and hydroxylases. Their composition is not only cell-specific but also strictly regulated during development and cell differentiation [50,51]. Since there exists evidence that ganglioside

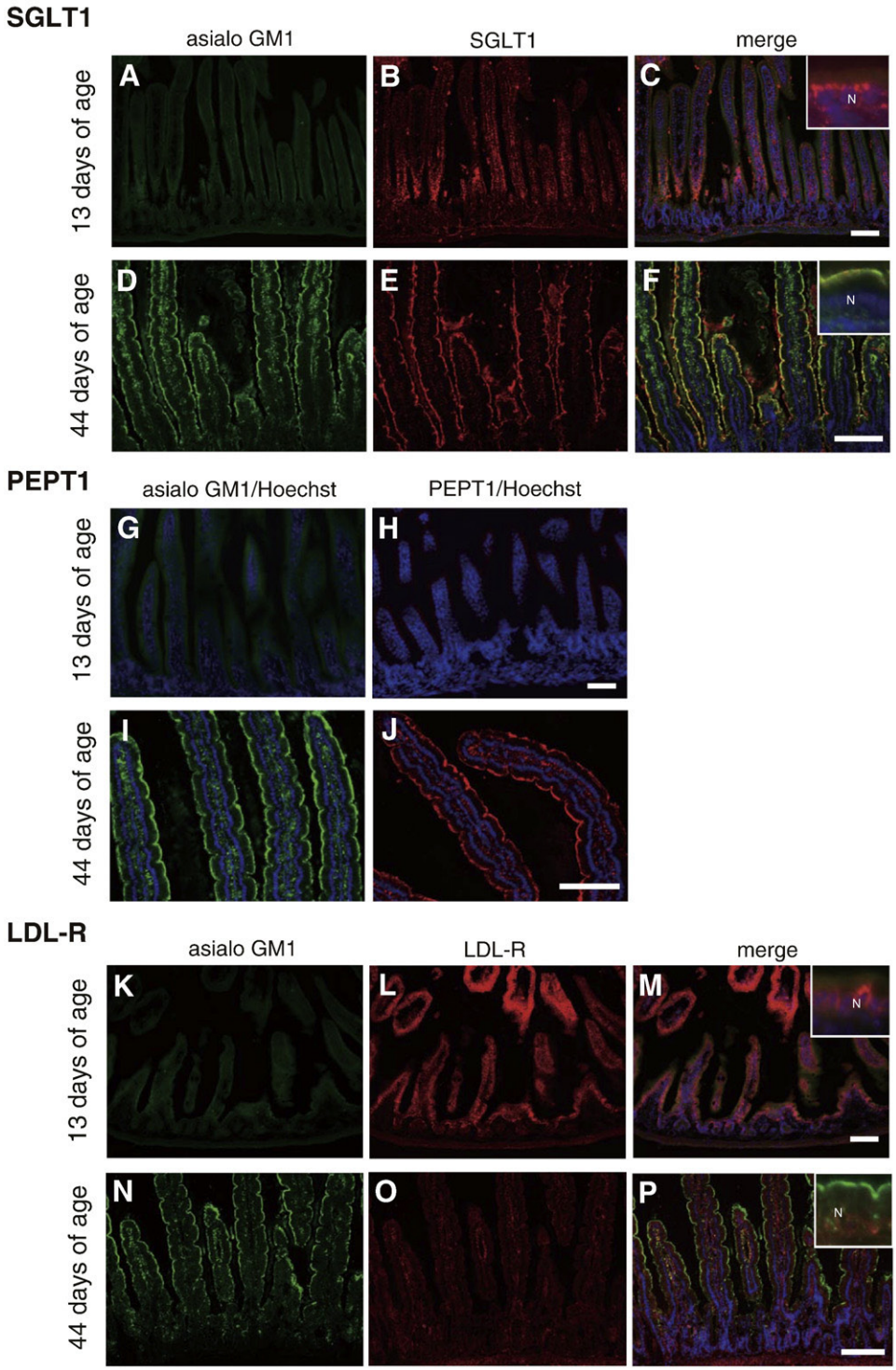

Fig. 7. Temporal immunohistochemical localization of nutrient transporters in the small intestine. For SGLT1, on day 13, immunoreactivity was detected mainly in the perinuclear area of epithelial cells. The intensity was less than that on day 44 (A–C). On day 44, immunoreactivity on the microvillous apical membrane of epithelial cells became intense. At the higher magnification panel inserted in (F), asialo GM1 and SGLT1 were colocalized on the microvillous apical membrane of epithelial cells (D–F). For PEPT1, on day 13, immunoreactivity of PEPT1 was hardly detected in epithelial cells (G and H). On day 44, the intense immunoreactivity of PEPT1 was observed on the microvillous apical membrane of epithelial cells (I and J). For LDL-R, immunoreactivity was more intense on day 13 (K–M) than on day 44 (N–P). It was detected on the basolateral membrane of epithelial cells and did not colocalize with asialo GM1 on day 44 (higher magnification panel inserted in L). Scale bars represent 100 μm.

biosynthesis is intimately regulated at the transcriptional level in most cases [52,53], the combinational and tissue-specific transcriptional down-regulation of GM3 synthase and Glb1 at around 2–3 weeks of age may cause the decrease in their protein levels and enzyme activities, followed by the induction of asialo GM1. To explore the factors that coordinately regulate the transcription of these enzymes, GM3 synthase and Glb1 in the small intestine are subjects of future research.

On the other hand, it is possible that the change in luminal content (breast milk to solid diet) influences the developmental changes in GSL composition in the small intestine. To test this possibility, we fed the mother mouse only with low-fat milk during the suckling-to-weaning period until 31 days and analyzed the developmental changes in GSL composition in her pups. In this experiment, pups have no chance of accessing the solid diet and are only fed mother's breast milk through the suckling-to-weaning period. Then we found that even in this situation, the GSL composition of these pups showed identical changes in GSL composition and conversion from GM1 and GM3 into asialo GM1 between 16 and 19 days, as seen in the pups that have free access to solid diet (data not shown). These data suggest that the conversion from GM1 and GM3 into asialo GM1 was mainly regulated by genetic factors, not by the luminal content of the small intestine.

What is the biological role of this developmental induction of asialo GM1 in the mouse small intestine? The mammalian small intestine undergoes important transformations in its structure, as well as in the way it absorbs nutrients during postnatal development [27]. Since gangliosides are suggested to regulate cell proliferation and differentiation, the increased sialylated gangliosides (GM3 and GM1) during the early neonatal period may play a role as a trophic factor for intestinal epithelial cells. In contrast, based on the immunohistochemical localization of asialo GM1 at the brush border membrane of epithelial cells (Fig. 4), asialo GM1 could be responsible for the transformation of the microvillous membrane or for supporting transporter protein functions in the brush border membrane. The elongation of microvilli is observed at around 2 weeks after birth in mice [27,54].

Several studies have demonstrated the postnatal changes in nutrient transporters in the small intestine at both mRNA and protein levels [55–58]. The present data for the mRNA expression of several nutrient transporters showed a distinct pattern of changes between 16 and 24 days of age, around which time the developmental changes in GSL composition occur. Some transporters (PEPT1, SGLT1, GLUT5 and NaDC-1) were significantly up-regulated, while several amino acid transporters (EAAT3, y+LAT-1 and ASC-1), GLUT2 and LDL-R were down-regulated. Although the changes in the mRNA levels of nutrient transporters may not equate to changes in protein levels or activities, the present data are basically compatible with previously reported information on the protein or activity levels of nutrient transporters [59,60]. These changes also seemed reasonable enough to account for the developmental changes in diet —from liquid milk during suckling, which is high in protein and lipids and low in carbohydrates, to a solid diet after weanling, which is generally low in lipids and protein and high in carbohydrates. In addition, the temporal changes in the immunohistochemical localization of SGLT1 in enterocytes, from the perinuclear region before 2 weeks of age to the distinct localization in the microvillous apical membrane and its colocalization with asialo GM1, also raise the possibility of the contribution of GSLs to the development of nutrient transporters.

The results described here suggest the importance of specific GSL molecular species for the structural and functional development of the intestinal brush border membrane. However, the physiological significance of GSLs for supporting transporter protein functions remains a matter of speculation. To delineate how these changes in GSL composition regulate nutrient transporters, further studies that manipulate specific GSL species using metabolic inhibitors and/or genetically engineered mice [61,62] will be required to determine whether the loss of specific GSLs will disrupt transporter expression and activity. Based on our present results, GM3 synthase knockout mice (as a model of GM3 and GM1 deficiency) and GM2 synthase knockout mice (as a model of asialo GM1 deficiency) will give us more definitive insights for addressing the physiological significance of GSLs to support transporter protein functions.

Acknowledgments

We thank Dr. Kyoko Nakamura and Dr. Yasuhiro Kuroda for helpful comments and technical assistance with TLC-MS analysis. This work was supported by the Japan Society for the Promotion of Sciences, Grant-in-aid for Scientific Research (18591169) and a grant for Research for Intractable Diseases from the Japanese Ministry of Health, Welfare, and Labor. J.M. was supported, in part, by a grant for Hi-Tech Research from Tokai University, Japan.

References

[1] Louvard D, Kedlinger M, Hauri HP. The differentiating intestinal epithelial cell: establishment and maintenance of functions through interactions between cellular structures. Annu Rev Cell Biol 1992;8:157–95.
[2] Crosnier C, Stamataki D, Lewis J. Organizing cell renewal in the intestine: stem cells, signals and combinatorial control. Nat Rev Genet 2006;7:349–59.
[3] Smith WL, Merrill Jr AH. Sphingolipid metabolism and signaling minireview series. J Biol Chem 2002;277:25841–2.
[4] Merrill Jr AH. De novo sphingolipid biosynthesis: a necessary, but dangerous, pathway. J Biol Chem 2002;277:25843–6.
[5] Simons K, Vaz WL. Model systems, lipid rafts, and cell membranes. Annu Rev Biophys Biomol Struct 2004;33:269–95.
[6] Füllekrug J, Simons K. Lipid rafts and apical membrane traffic. Ann NY Acad Sci 2004;1014:164–9.
[7] Hakomori S. Bifunctional role of glycosphingolipids. Modulators for transmembrane signaling and mediators for cellular interactions. J Biol Chem 1990;265:18713–6.
[8] Endo K, Akiyama T, Kobayashi S, Okada M. Degenerative spermatocyte, a novel gene encoding a transmembrane protein required for the initiation of meiosis in *Drosophila* spermatogenesis. Mol Gen Genet 1996;253:157–65.
[9] Endo K, Matsuda Y, Kobayashi S. Mdes, a mouse homolog of the *Drosophila* degenerative spermatocyte gene is expressed during mouse spermatogenesis. Dev Growth Differ 1997;39:399–403.
[10] Ternes P, Franke S, Zahringer U, Sperling P, Heinz E. Identification and characterization of a sphingolipid Δ^4-desaturase family. J Biol Chem 2002;277:25512–8.
[11] Omae F, Miyazaki M, Enomoto A, Suzuki M, Suzuki Y, Suzuki A. DES2 protein is responsible for phytoceramide biosynthesis in the mouse small intestine. Biochem J 2004;379:687–95.
[12] Enomoto A, Omae F, Miyazaki M, Kozutsumi Y, Yubisui T, Suzuki A. Dihydroceramide:sphinganine C-4-hydroxylation requires Des2 hydroxylase and the membrane form of cytochrome *b*5. Biochem J 2006;397:289–95.
[13] Eckhardt M, Yaghootfam A, Fewou SN, Zöller I, Gieselmann V. A mammalian fatty acid hydroxylase responsible for the formation of alpha-hydroxylated galactosylceramide in myelin. Biochem J 2005;388:245–54.
[14] Alderson NL, Rembiesa BM, Walla MD, Bielawska A, Bielawski J, Hama H. The human FA2H gene encodes a fatty acid 2-hydroxylase. J Biol Chem 2004;279:48562–8.
[15] Hakomori S. Structures and organization of cell surface glycolipids dependency on cell growth and malignant transformation. Biochim Biophys Acta 1975;417:55–89.
[16] Iwamori M, Nagai Y. GM3 ganglioside in various tissues of rabbit. Tissue-specific distribution of *N*-glycolylneuraminic acid-containing GM3. J Biochem 1978;84:1609–15.
[17] Breimer ME, Hansson GC, Karlsson KA, Leffler H. Blood group type glycosphingolipids from the small intestine of different animals analysed by mass spectrometry and thin-layer chromatography. A note on species diversity. J Biochem 1981;90:589–609.
[18] Umesaki Y, Suzuki A, Kasama T, Tohyama K, Mutai M, Yamakawa T. Presence of asialo GM_1 and glucosylceramide in the intestinal mucosa of mice and induction of fucosyl asialo GM_1 by conventionalization of germ-free mice. J Biochem (Tokyo) 1981;90:1731–8.
[19] Suzuki A, Yamakawa T. The different distribution of asialo GM_1 and Forssman antigen in the small intestine of mouse demonstrated by immunofluorescence staining. J Biochem (Tokyo) 1981;90:1541–4.
[20] Suzuki A, Umesaki Y, Yamakawa T. Localization of asialo GM_1 and Forssman antigen in the small intestine of mouse. Adv Exp Med Biol 1982;152:415–24.
[21] Smith EL, McKibbin JM, Karlsson KA, Pascher I, Samuelsson BE. Characterization by mass spectrometry of blood group A active glycolipids from human and dog small intestine. Biochemistry 1975;10:2120–4.
[22] Bouhours JF, Glickman RM. Rat intestinal glycolipids: III. Fatty acids and long chain bases of glycolipids from villus and crypt cells. Biochim Biophys Acta 1977:51–60.
[23] Breimer ME, Hansson GC, Karlsson KA, Leffler H. Studies on differentiating epithelial cells of rat small intestine: alterations in the lipophilic part of glycosphingolipids during cell migration from crypt to villus tip. Biochim Biophys Acta 1982;710:415–27.

[24] Breimer ME, Falk KE, Hansson GC, Karlsson KA. Structural identification of two ten-sugar branched chain glycosphingolipids of blood group H type present in epithelial cells of rat small intestine. J Biol Chem 1982;257:50–9.
[25] McKibbin JM, Spencer WA, Smith EL, Mansson JE, Karlsson KA, Samuelsson BE, et al.. Lewis blood group fucolipids and their isomers from human and canine intestine. J Biol Chem 1982;257:755–60.
[26] Dahiya R, Brown MD, Brasitus TA. Distribution of glycosphingolipids of monkey small and large intestinal mucosa. Lipids 1986;21:107–11.
[27] Moog F. Development of mammalian absorptive processes, Ciba Foundation Series 70. , Amsterdam: Elsevier; 1979. p. 31–50.
[28] Fujita N, Suzuki K, Vanier MT, Popko B, Maeda N, Klein A, et al.. Targeted disruption of the mouse sphingolipid activator protein gene: a complex phenotype, including severe leukodystrophy and wide-spread storage of multiple sphingolipids. Hum Mol Genet 1996;5:711–25.
[29] Kyrklund T. Two procedures to remove polar contaminants from a crude brain lipid extract by using prepacked reversed-phase columns. Lipids 1987;22:274–7.
[30] Matsuda J, Vanier MT, Saito Y, Tohyama J, Suzuki K, Suzuki K. A mutation in the saposin A domain of the sphingolipid activator protein (prosaposin) gene causes a late-onset, slowly progressive form of globoid cell leukodystrophy in the mouse. Hum Mol Genet 2001;10:1191–9.
[31] Abramson MB, Norton WT, Katzman R. Study of ionic structures in phospholipids by infrared spectra. J Biol Chem 1965;240:2389–95.
[32] Nakamura K, Suzuki Y, Goto-Inoue N, Yoshida-Noro C, Suzuki A. Structural characterization of neutral glycosphingolipids by thin-layer chromatography coupled to matrix-assisted laser desorption/ionization quadrupole ion trap time-of-flight MS/MS. Anal Chem 2006;78:5738–43.
[33] Miyazaki M, Yoneshige A, Matsuda J, Kuroda Y, Kojima N, Suzuki A. HPTLC-MS for rapid analysis of neutral glycosphingolipids. J AOAC Int 2008;91:1218–26.
[34] Tominaga K, Matsuda J, Kido M, Naito E, Yokota I, Toida K, et al.. Genetic background markedly influences vulnerability of the hippocampal neuronal organization in the “twitcher” mouse model of globoid cell leukodystrophy. J Neurosci Res 2004;77:507–16.
[35] Umesaki Y, Tohyama K, Mutai M. Appearance of fucolipid after conventionalization of germ-free mice. J Biochem 1981;90:559–61.
[36] Umesaki Y, Takamizawa K, Ohara M. Structural and compositional difference in the neutral glycolipids between epithelial and non-epithelial tissue of the mouse small intestine. Biochim Biophys Acta 1989;1001:157–62.
[37] Umesaki Y. Immunohistochemical and biochemical demonstration of the change in glycolipid composition of the intestinal epithelial cell surface in mice in relation to epithelial cell differentiation and bacterial association. J Histochem Cytochem 1984;32:299–304.
[38] Domon B, Costello CE. Structure elucidation of glycosphingolipids and gangliosides using high-performance tandem mass spectrometry. Biochemistry 1988;27:1534–43.
[39] Hsu FF, Turk J, Stewart ME, Downing DT. Structural studies on ceramides as lithiated adducts by low energy collisional-activated dissociation tandem mass spectrometry with electrospray ionization. J Am Soc Mass Spectrom 2002;13:680–95.
[40] Bouhours JF, Glickman RM. Rat intestinal glycolipids: II. Distribution and biosynthesis of glycolipids and ceramide in villus and crypt cells. Biochim Biophys Acta 1976;441:123–33.
[41] Glickman RM, Bouhours JF. Characterization, distribution and biosynthesis of the major ganglioside of rat intestinal mucosa. Biochim Biophys Acta 1976;424:17–25.
[42] Umesaki Y, Sakata T, Yajima T. Abrupt induction of GDP-fucose: asialo GM1 fucosyltransferase in the small intestine after conventionalization of germ-free mice. Biochem Biophys Res Commun 1982;105:439–43.
[43] Umesaki Y, Ohara M. Factors regulating the expression of the neutral glycolipids in the mouse small intestinal mucosa. Biochim Biophys Acta 1989;1001:163–8.
[44] Bouhours D, Bouhours JF. Developmental changes of rats intestinal glycolipids. Biochem Biophys Res Commun 1981;99:1384–9.
[45] Bouhours D, Bouhours JF. Developmental changes of hematoside of rat small intestine: postnatal hydroxylation of fatty acids and sialic acid. J Biol Chem 1983;258:299–304.
[46] Bouhours JF, Bouhours D, Hansson GC. Developmental changes of glycosphingolipid composition of epithelia of rat digestive tract. Adv Lipid Res 1993;26:353–72.
[47] Sato E, Uezato T, Fujita M, Nishimura K. Developmental profiles of glycolipids in mouse small intestine. J Biochem 1982;91:2013–9.
[48] Sato E, Fujie M, Uezato T, Fujita M, Nishimura K. Hormonal effects on the development changes of mouse small intestinal glycolipids. Biochem Biophys Res Commun 1984;119:1168–73.
[49] Biol-N'garagba MC, Louisot P. Regulation of the intestinal glycoprotein glycosylation during postnatal development: role of hormonal and nutritional factors. Biochimie 2003;85:331–52.
[50] Tsuji S. Molecular cloning and functional analysis of sialyltransferases. J Biochem 1996;120:1–13.
[51] Yu RK, Bieberich E, Xia T, Zeng G. Regulation of ganglioside biosynthesis in the nervous system. J Lipid Res 2004;45:783–93.
[52] Zeng G, Yu RK. Cloning and transcriptional regulation of genes responsible for synthesis of gangliosides. Curr Drug Targets 2008;9:317–24.
[53] Xia T, Zeng G, Gao L, Yu RK. Sp1 and AP2 enhance promoter activity of the mouse GM3-synthase gene. Gene 2005;351:109–18.
[54] Sato T, Mushiake S, Kato Y, Sato K, Sato M, Takeda N, et al.. The Rab8 GTPase regulates apical protein localization in intestinal cells. Nature 2007;448:366–9.
[55] Kim HR, Park SW, Cho HJ, Chae KA, Sung JM, Kim JS, et al.. Comparative gene expression profiles of intestinal transporters in mice, rats and humans. Pharmacol Res 2007;56:224–36.
[56] Hui DY, Labonté ED, Howles PN. Development and physiological regulation of intestinal lipid absorption: III. Intestinal transporters and cholesterol absorption. Am J Physiol Gastrointest Liver Physiol 2008;294:G839–43.
[57] Toloza EM, Diamond J. Ontogenetic development of nutrient transporters in rat intestine. Am J Physiol 1992;263:G593–604.
[58] Buddington RK. Intestinal nutrient transport during ontogeny of vertebrates. Am J Physiol 1992;263:R503–9.
[59] Pacha J. Development of intestinal transport function in mammals. Physiol Rev 2000;80:1633–67.
[60] Ferraris RP. Dietary and developmental regulation of intestinal sugar transport. Biochem J 2001;360:265–76.
[61] Takamiya K, Yamamoto A, Furukawa K, Yamashiro S, Shin M, Okada M, et al.. Mice with disrupted GM2/GD2 synthase gene lack complex gangliosides but exhibit only subtle defects in their nervous system. Proc Natl Acad Sci U S A 1996;93:10662–7.
[62] Yamashita T, Hashiramoto A, Haluzik M, Mizukami H, Beck S, Norton A, et al.. Enhanced insulin sensitivity in mice lacking ganglioside GM3. Proc Natl Acad Sci U S A 2003;100:3445–9.